JOURNAL OF MATERIALS SCIENCE 10 (1975) 1591–1602

# A scanning electron microscopic study of hybrid composite impact response

DONALD F. ADAMS*
*Department of Mechanical Engineering, University of Wyoming, Laramie, Wyoming, USA*

Scanning electron micrographs of fracture surfaces of various hybrid composite materials subjected to Charpy impact tests are presented. Macrophotographs of the failed specimens which indicate the gross failure modes, and actual impact load–time traces obtained using an instrumented tup impact test technique are also included. These data permit a direct comparison between observed microfailure modes and the gross response of each composite to failure. An all-graphite/epoxy control configuration and three hybrid configurations are considered. The third-phase fibre additions in these hybrids include glass, Kevlar 49, and Nomex nylon. Longitudinal and transverse impact tests of both notched and unnotched standard Charpy specimens are included, for both a basic unidirectional graphite/epoxy composite and a quasi-isotropic laminate orientation.

## 1. Introduction

Graphite-fibre-reinforced epoxy matrix composites are among the highest static strength and stiffness materials available at the present time, and their low density makes them particularly attractive for use in weight-critical systems. However, the potential of graphite/epoxy composites in many structural applications has been hindered to date by the very low impact strengths which they characteristically exhibit.

One method of alleviating this problem is to combine a high static properties graphite/epoxy composite with another material which exhibits a high impact strength. One such material is glass-fibre-reinforced epoxy which, while also having excellent strength characteristics, has a relatively low stiffness. By constructing a laminate of alternating thin plies of these two composite materials, a required balance of static and impact properties can be achieved. Such a laminate, containing a third material phase such as glass fibres, is termed a hybrid composite. A number of other third-phase materials have also been utilized [1-3].

The primary role of the third-phase material is to alter the failure mode of the graphite/epoxy composite. A graphite/epoxy composite typically fails in a "brittle" manner, i.e. the fracture surface is relatively smooth. Much more fracture energy can be dissipated in a fibre-reinforced composite by promoting fibre-matrix interface debonding (creation of new free surface), fibre pull-out, delamination, etc. Considering that typical fibre diameters are in the 6 to 8 μm range, the study of these fracture modes and energy dissipation mechanisms is truly a micromechanical analysis.

A scanning electron microscope was used in the present investigation to provide the required detail information relating to the failure mechanism modifications achieved by the introduction of various third-phase materials.

## 2. Specimen configurations

A standard Charpy impact specimen geometry was utilized, namely a beam 5.5 cm (2.16 in.) long and 1.0 cm (0.394 in.) square in cross-section. The beam was oriented in the testing machine such that the impact force was applied normal to the plane of the laminae. Both unnotched and notched specimens were tested, the notched specimens containing a standard Charpy V-notch, 0.2 cm (0.079 in.) deep.

The fracture mode of an individual lamina or ply of a laminated composite material is strongly influenced by the relative orientations of adjacent plies. Each ply is highly anisotropic, consisting of a thin layer of fibres all oriented in

*Also consultant to Aeronutronic Division, Philco-Ford Corporation, Newport Beach, California.

TABLE I Fibre material properties

| Property | Fibre material | | | | |
|---|---|---|---|---|---|
| | | Modmor II graphite | Glass ECG 150–1/0 | Kevlar 49 type III | Nomex nylon |
| Tensile strength: | GN $m^{-2}$ | 2.48 | 4.58 | 2.76 | 0.65 |
| | ($10^3$ lb $in^{-2}$) | (360) | (665) | (400) | (94) |
| Tensile modulus: | GN $m^{-2}$ | 269 | 86.9 | 131 | 15.9 |
| | ($10^6$ lb $in^{-2}$) | (39) | (12.6) | (19) | (2.3) |
| Elongation: | % | 0.9 | 5.4 | 2.0 | 22.0 |
| Density: | g $cm^{-3}$ | 1.71 | 2.49 | 1.45 | 1.38 |
| Denier: | g/9000 m | 7830 | 304 | 195 | 200 |

one direction and impregnated with an epoxy polymer matrix material. Two basic graphite/epoxy ply lay-up configurations were investigated: a unidirectional system in which all of the graphite/epoxy plies were oriented in one direction, and a quasi-isotropic system in which the plies were oriented in a 0°, ± 45°, 90° lay-up sequence. These configurations represent the extremes of laminate anisotropy which can be achieved.

Modulite 5206 graphite/epoxy prepreg was used. Produced by the Whittaker Corporation-Narmco Materials Division, this material consists of their Modmor II graphite fibres impregnated with Narmco 1004 epoxy matrix. The properties of the Modmor II fibres are given in Table I.

These basic graphite/epoxy laminates were hybridized by interleaving unidirectional plies of three different fibre/epoxy composites, namely glass, Kevlar 49, and nylon fibres impregnated with the same Narmco 1004 epoxy matrix. The properties of these third-phase fibres are also given in Table I. The high-modulus glass fibres are produced by Owens-Corning Corporation. Kevlar 49 is a high-modulus organic fibre produced by the DuPont Corporation, and was designated as PRD-49 in their earlier marketing and development work. Nomex is a nylon fibre produced by DuPont. These three fibres were selected as representing a wide range of mechanical properties including, in particular, elongation.

In the unidirectional Modulite 5206 graphite/epoxy laminates, the third-phase fibre plies were interleaved at alternating + 45° and − 45° orientations throughout the thickness, each third-phase ply being spaced between four Modulite 5206 plies. These were defined as type A hybrid composites.

In the quasi-isotropic Modulite 5206 laminates, the third-phase fibre plies were interleaved at a 0° orientation throughout the thickness, separating + 45°, 90°, 0°, − 45° sets of Modulite 5206 plies. These were defined as type B hybrid composites.

For comparison purposes, laminates containing only Modulite 5206 plies, but laid-up in the same type A and type B orientations as the hybrids, were also tested. These are referred to as the Modulite 5206 control laminates, or the 5206/5206 systems.

## 3. Impact testing

Since both the type A and the type B laminates were highly anisotropic, impact testing was conducted on both longitudinal and transverse impact specimens. The longitudinal impact specimens were defined as those having the 0° plies oriented along the longitudinal beam axis of the Charpy specimen; the transverse impact specimens had the 0° plies oriented perpendicular or transverse to the axis of the Charpy specimen.

A Dynatup Instrumented Impact Test System, developed by Effects Technology, Inc, Santa Barbara, California, was used in conducting all of the impact testing in the present study. This instrumentation package was utilized in conjunction with a standard 1068 J (240 ft-lb) capacity, pendulum-type, Riehle impact tester. The instrumented test apparatus is designed to display a load versus time curve while simultaneously integrating the area under the curve to provide a cumulative absorbed energy trace. The apparatus actually records the instantaneous impact load that is acting on a strain-gauge load cell mounted on the striker head of the impact tester. The load and energy traces were displayed on a Tektronix storage oscilloscope. The image was then photographed to provide a permanent

TABLE II Total impact energy of various laminated composites*

| Material system | Laminate type | Impact orientation | Total impact energy† kJ m$^{-2}$ (ft–lb in$^{-2}$.) | | | |
|---|---|---|---|---|---|---|
| | | | Unnotched | | Notched | |
| 5206/5206 | A | longitudinal | 111 | (53) | 113 | (54) |
| | | transverse | 21 | (10) | 23 | (11) |
| | B | longitudinal | 84 | (40) | 92 | (44) |
| | | transverse | 69 | (33) | 69 | (33) |
| 5206/Glass | A | longitudinal | 122 | (58) | 120 | (57) |
| | | transverse | 36 | (17) | 38 | (18) |
| | B | longitudinal | 294 | (140) | 273 | (130) |
| | | transverse | 86 | (41) | 57 | (27) |
| 5206/Kevlar 49 | A | longitudinal | 95 | (45) | 88 | (42) |
| | | transverse | 40 | (19) | 34 | (16) |
| | B | longitudinal | 181 | (86) | 141 | (67) |
| | | transverse | 80 | (38) | 78 | (37) |
| 5206/Nomex | A | longitudinal | 82 | (39) | 84 | (40) |
| | | transverse | 8 | (4) | 8 | (4) |
| | B | longitudinal | 53 | (25) | 53 | (25) |
| | | transverse | 50 | (24) | 50 | (24) |

*Average of three tests.
†Normalized by dividing by specimen cross-sectional area.

record for subsequent measurements and studies of the load and energy histories.

Several of these photographs are included in this paper. The manner in which the impact force varies during the fracture process provides additional information for use in determining the failure modes occurring at the micromechanical level. These observations can be correlated both with the SEM observations and the gross deformations of the failed impact specimens. Post-impact photographs of several specimens are also included in this paper.

A total of three specimens of each of the many configurations were tested and the results averaged. A tabulation of the average total impact energies obtained is presented in Table II. Although all impact specimens were nominally of the same dimensions, the presence of the notch in the notched specimens reduced their cross-sectional area at the fracture plane. To account for this difference in net area between the notched and unnotched specimens, all impact energy values have been normalized by dividing by the actual cross-sectional area.

Since complete impact force-time and impact energy-time traces were available from the instrumented impact tests, many additional data were available also. Additional impact energy results are presented and discussed in detail in [1] and [3].

## 4. Scanning electron microscopy

All scanning electron microscopy (SEM) work was done using the University of Wyoming's JELCO JSM-U3 unit (Japan Electron Optics Laboratory Co, Inc). A total of fifteen impact specimen fracture surfaces were examined in detail. The fracture surfaces were vapour-coated with a thin layer of gold to enhance the image. Unless otherwise noted, all SEM photographs were taken at an angle of 45° with respect to the fracture surface, so that a ply of the composite laminate having a 0° orientation with respect to the specimen longitudinal axis appears to be tilted at an angle of 45° to the right in the photographs. Also, all photographs are oriented such that the photographed area of the specimen which was nearest to the tension side of the impact specimen is at the top of the photograph.

## 5. SEM observations

The following general discussion emphasizes the most important of the features observed, and includes only a small number of the total observations made.

### 5.1. Modulite 5206 control laminates

The all-graphite/epoxy control materials, both type A and type B laminates and both notched and unnotched specimens, all failed in essentially the same manner. A photograph of a typical failed Charpy impact specimen is shown in Fig. 1. The corresponding instrumented impact load–time trace for this specimen is also shown. This and the several other traces included in

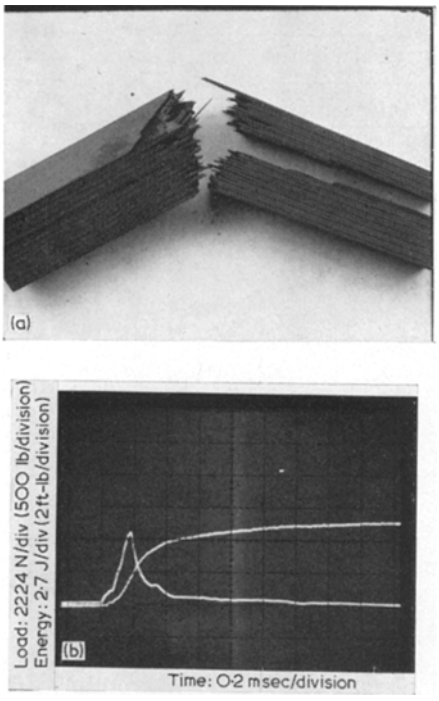


*Figure 1* Modulite 5206 control laminate, lay-up B, longitudinal impact, unnotched specimen. (a) failed impact specimen, tension side at top; (b) instrumented impact load and energy waveforms.

certain of the figures of this section are discussed in Section 6. The failed specimen indicates a single gross delamination through the right half of the specimen and an indication of a partial delamination in the left half. Some specimens exhibited a complete delamination through both halves, while others contained no gross delaminations at all. However, the actual primary fracture surface differed little in appearance from one specimen to another. A relatively brittle fracture is indicated. The individual plies and their orientations can be observed in Fig. 1.

Fig. 2 is an SEM photograph of an area of a 0° ply of the specimen of Fig. 1. Being a longitudinal impact specimen, the 0° plies are oriented parallel to the beam axis and they carried a large part of the impact load. Fig. 2 is typical of all the 0° plies at the fracture surface, both those which would also be graphite/epoxy in the type B hybrid system, and those which here replaced the third-phase plies. The 0° plies of the type A, longitudinal impact specimens had a similar appearance. Also, there was no apparent variation in the fracture mode from the tension to the compression side of the impact specimens. Fig. 2

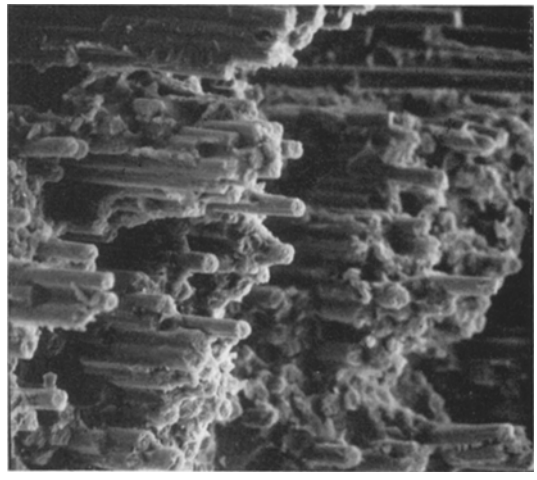

*Figure 2* Modulite 5206 control laminate, lay-up B, longitudinal impact, unnotched specimen: SEM observation of 0° ply near compression side of specimen, × 450.

happens to have been taken in a region near the compression side.

In general, the control laminates exhibited relatively little pull-out of individual fibres or bundles of fibres, there being large areas of almost smooth fracture surface. The + 45° and − 45° plies indicated even less pull-out, a very distinct cleavage fracture being observed.

Neither type A nor type B laminates exhibited notch sensitivity in terms of total impact energy (see Table II), and there was no observable difference in the gross failure mode nor in the SEM examinations at the microlevel.

### 5.2. Modulite 5206/glass hybrid-type A laminates

The total impact energies of the various specimen configurations of this hybrid were approximately the same as those of the Modulite 5206, type A control laminates, as indicated in Table II. Type A hybrids were much less effective than type B hybrids. The gross failure mode was a pull-out of the glass plies; the individual glass fibres did not fail.

A photograph of a failed longitudinal impact specimen is shown in Fig. 3. This happens to be a notched specimen, although the unnotched specimens failed in essentially the same manner. Some specimens did exhibit more than one gross delamination, however. A failed unnotched transverse impact specimen is shown in Fig. 4. The pull-out of the glass plies is readily apparent. The notched specimens looked the same.

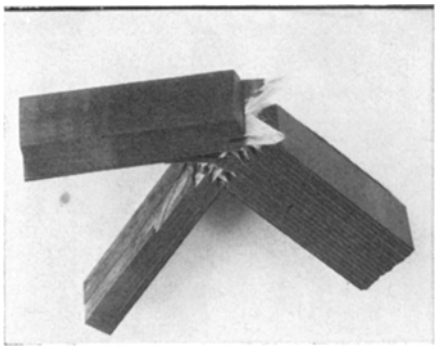

*Figure 3* Modulite 5206/glass hybrid, lay-up A, longitudinal impact, notched specimen.

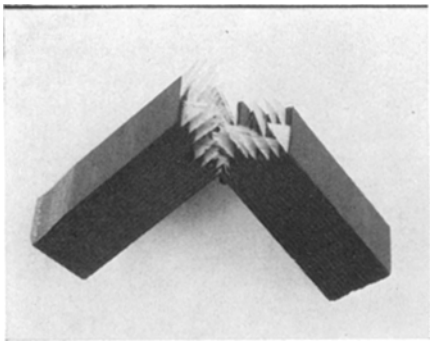

*Figure 4* Modulite 5206/glass hybrid, lay-up A, transverse impact, unnotched specimen.

Fig. 5 is a low magnification SEM of a 0° graphite/epoxy ply in an unnotched, longitudinal impact specimen. It shows the failure mode in the 0° graphite/epoxy ply nearest the tension surface. The fibre pull-out lengths are relatively small, and a considerable number of matrix particles can be observed still adhering to the fibre surfaces. Fig. 5 also shows a fibre bundle which has been partially broken away and bent toward the compression side of the specimen. This was a very common occurrence on the tension side of the specimen and probably represents the effect of a relative sliding motion between specimen halves during the very late stages of the impact process. The 0° graphite/epoxy plies located near the compression surface of the specimen indicated almost no individual fibre pull-out and very smooth cleavage failure. Some bending of partially failed bundles was noted, similar to that on the tension side (Fig. 5) and in the same direction.

In addition to the distinct difference in overall failure mode between the tension and the

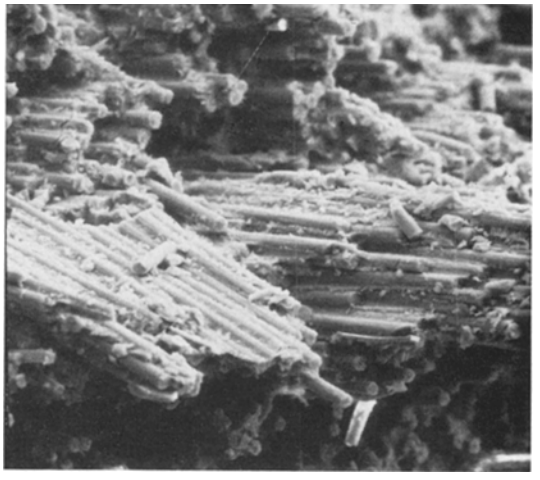

*Figure 5* Modulite 5206/glass hybrid, lay-up A, longitudinal impact, unnotched: 0° graphite/epoxy ply near tension surface showing broken fibre bundle, × 300.

compression side, there was also a difference in appearance of the fractured ends of individual graphite fibres. A ×3500 magnification of individual fibres on the compression side is shown in Fig. 6. The half of each fibre nearest the

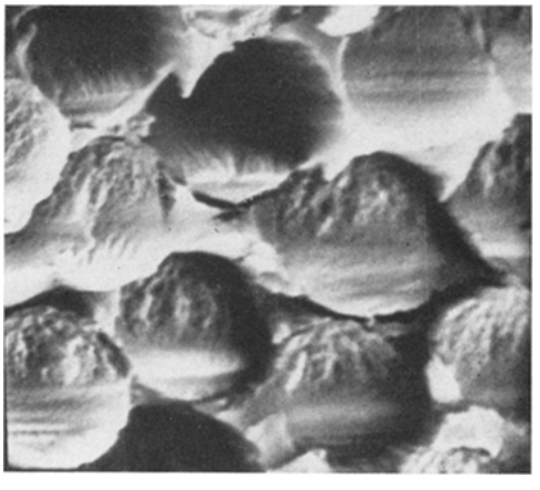

*Figure 6* Modulite 5206/glass hybrid, lay-up A, longitudinal impact, unnotched: 0° graphite/epoxy ply near compression surface, × 3500.

tension side of the specimen (the top half of each fibre in Fig. 6) is of coarse texture, typical of a tensile failure. However, the lower half is relatively smooth with some horizontal striations, indicating the probability of a shear (compressive) failure. It is suspected that this was caused by the lower plies of material having

delaminated during the impact process, and then the resulting thin plate being bent severely to failure during the final stage of fracture, i.e., it is suspected that this rather unique observation is not a significant fracture in itself, but rather that it is a symptom of the gross delamination which typically occurred in these materials. This mode of fibre failure did not occur on the tension side (where initial failure probably occurred).

In lay-up A, transverse impact specimens such as shown in Fig. 4, the glass epoxy plies, oriented at + 45° and − 45° angles to the beam axis, all pulled out without fibre failure. The graphite fibres, being all oriented normal to the beam axis in this transverse impact test, were not axially loaded. That is, the graphite plies were subjected to transverse impact. Fig. 7 shows a typical

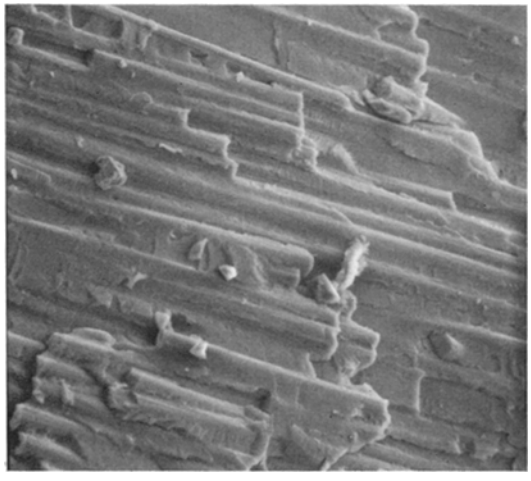

*Figure 7* Modulite 5206/glass hybrid, lay-up A, transverse impact, unnotched: 0° graphite/epoxy ply, × 450.

failure surface of a graphite/epoxy ply. Essentially no fibres were exposed, the failure occurring almost exclusively in the epoxy matrix. This indicates a good fibre–matrix interface bond. No difference was apparent in going from the tension to the compression side of the specimen.

### 5.3. Modulite 5206/glass hybrid-type B laminates

Type B Modulite 5206/glass hybrid laminates resulted in a much greater improvement in impact energy absorption relative to type B all-graphite/epoxy control laminates, as indicated in Table II, than did type A laminates when compared to type A control laminates. Yet the micromechanical failure mechanisms observed in the SEM study were representative of those normally associated with low energy absorption, i.e. cleavage fractures of the individual plies. There was little pull-out of fibres or bundles of fibres.

*Figure 8* Modulite 5206/glass hybrid, lay-up B, longitudinal impact, unnotched: 0° graphite/epoxy ply near tension surface, × 1750.

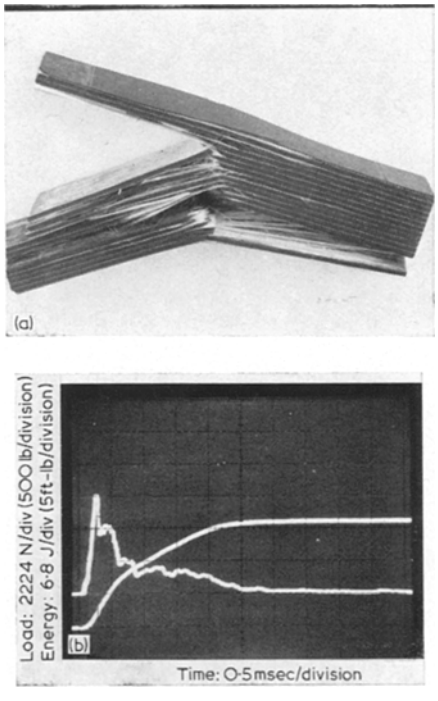


*Figure 9* Modulite 5206/glass hybrid, lay-up B, longitudinal impact, unnotched specimen. (a) Failed impact specimen, tension side at top; (b) instrumented impact load and energy waveforms.

Fig. 8 shows a region of a 0° ply of Modulite 5206 near the tensile surface of the unnotched, longitudinal impact specimen pictured in Fig. 9. As indicated in Fig. 9, most of the glass fibres in the glass/epoxy hybridizing plies (all oriented at 0° in a type B laminate) did not break; the specimen deformed sufficiently as a consequence of the multiple delaminations to slip off the supports. The SEM specimens were prepared by cutting the glass fibres with a razor blade to expose the fractured graphite/epoxy plies. Fig. 8 is non-typical of the 0° graphite/epoxy plies in that a region was selected which showed a maximum amount of fibre pull-out. Most of the fracture surface was completely featureless. The + 45° and − 45° plies exhibited a similar behaviour. There was no observed change in failure mode from the tension to the compression side of the specimen.

The notched, but otherwise identical, transverse impact specimens exhibited the same type of gross failure as is indicated for the unnotched specimen in Fig. 10, with no decrease in impact energy absorption, and no difference in fracture at the microlevel, not even in the graphite/epoxy plies right at the root of the notch.

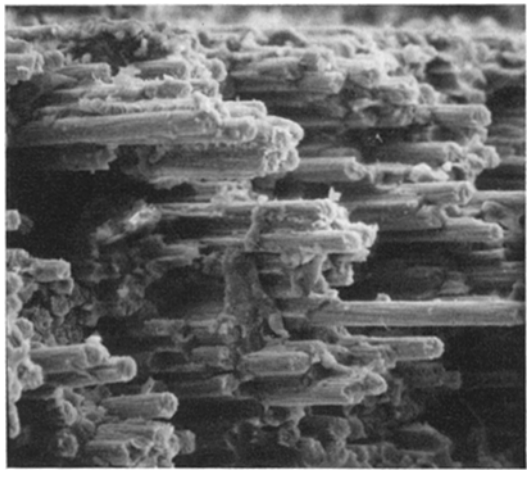

*Figure 10* Modulite 5206/glass hybrid, lay-up B, transverse impact, unnotched: 90° graphite/epoxy ply, tension region, × 450.

The general behaviour observed in the longitudinal impact specimens did not hold true in the transverse impact specimens, however. Since in the transverse impact specimens the third-phase reinforcement plies were oriented transverse or perpendicular to the beam axis and hence to the bending stresses, it could be anticipated that there would be little improvement in impact energy absorption relative to the type B, all-graphite/epoxy laminate. Basically this was true, as the results of Table II indicate. However, even though the impact energies were of the same magnitude, there was a distinct notch sensitivity exhibited; 86 kJ $m^{-2}$ (41 ft-lb $in^{-2}$) average total energy absorption for the three unnotched specimens versus 57 kJ $m^{-2}$ (27 ft-lb $in^{-2}$) for the notched specimens.

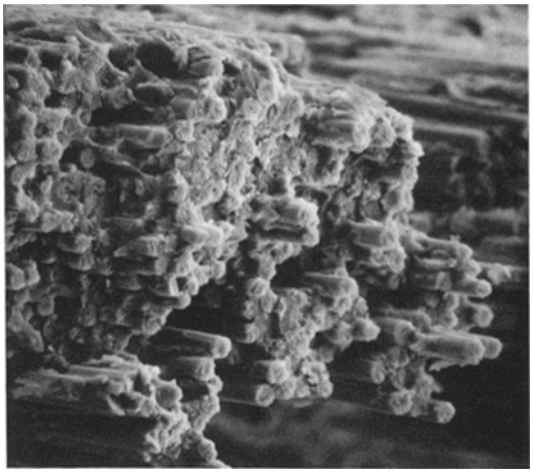

*Figure 11* Modulite 5206/glass hybrid, lay-up B, transverse impact, unnotched: 90° graphite/epoxy ply, compression region, × 450.

In spite of the apparent notch sensitivity of the transverse impact specimens, a study of the fracture modes of the graphite/epoxy plies indicated no observable difference. Fig. 10 is typical of the fracture surface almost everywhere on the tension side of these specimens, including the area right at the notch root of the notched specimens. The tension edge of the specimen can be seen at the top of Fig. 10. Although the fibre and bundle pull-out is not great, it is clearly much more pronounced than for the longitudinal impact specimens, as previously observed in Fig. 8. Also unlike the longitudinal impact specimens, there was a difference in appearance between the tension and compression sides of the fracture surface. In both the unnotched and notched specimens there was a tendency toward less fibre pull-out and more bundle pull-out on the compression side, as indicated in Fig. 11.

An interesting anomaly was noted in one of the specimens, however. Fig. 10 shows a typical

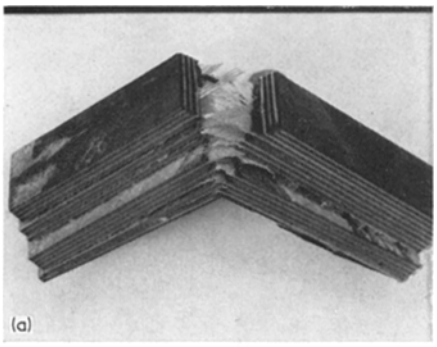


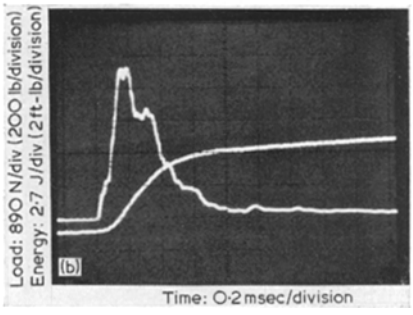


*Figure 12* Modulite 5206/Kevlar 49 hybrid, lay-up A, longitudinal impact, notched specimen. (a) Failed impact specimen, tension side at top. (b) instrumented impact load and energy waveforms.

fracture mode at the tensile surface. At one end of this tensile surface, a layer of material perhaps six to eight plies thick had delaminated locally from the remainder of the specimen. In this local region the failure mode was similar to that indicated in Fig. 11, i.e. a tendency toward a cleavage mode of failure. The reason for this change in failure mode is not completely clear, but seems to be associated with the change in stress state induced by the delamination. For example, this observed local failure mode tended toward the general cleavage mode observed in the longitudinal impact specimens (Fig. 8), where extensive gross delaminations occurred (Fig. 9).

### 5.4. Modulite 5206/Kevlar 49 hybrid-type A laminates

Fig. 12 shows a typical longitudinal impact specimen. The longitudinal impact specimens, whether notched or unnotched, exhibited extensive delamination, as the notched specimen of Fig. 12 shows. The transverse impact specimens did not delaminate, although the fracture surfaces looked about the same as indicated in Fig. 12. The Kevlar 49/epoxy hybridizing plies, oriented at + 45° and − 45°, pulled out as complete plies over a considerable length in both the longitudinal and transverse specimens. Most of the Kevlar 49 fibres did not fail; thus, there was little of interest to observe in the Kevlar 49/epoxy plies.

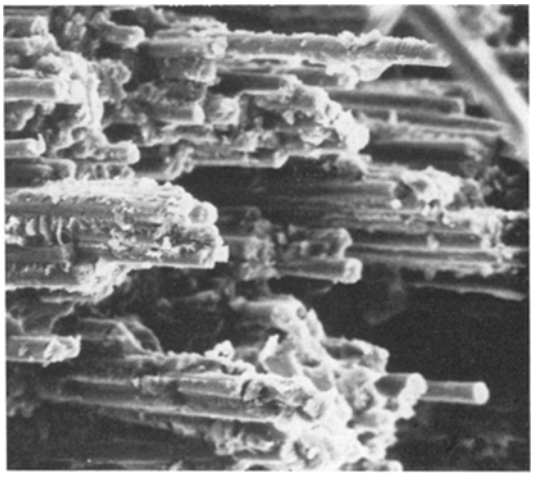

*Figure 13* Modulite 5206/Kevlar 49 hybrid, lay-up A, longitudinal impact, unnotched: near tension surface, × 425.

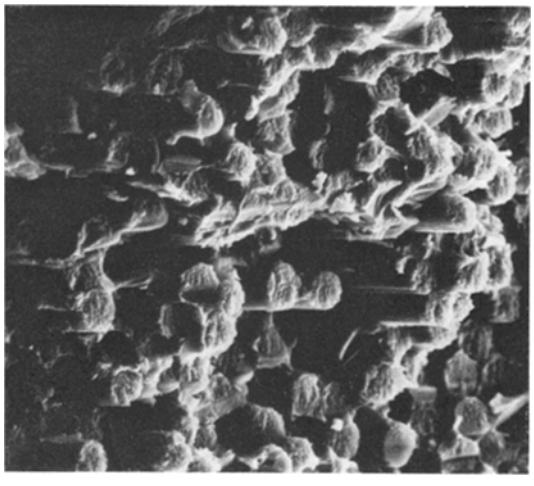

*Figure 14* Modulite 5206/Kevlar 49 hybrid, lay-up A, longitudinal impact, unnotched: 0° graphite/epoxy ply, near centre of specimen, × 1000.

The failure of the graphite/epoxy plies near the tension surface of the longitudinal impact specimens exhibited a considerable amount of fibre bundle pull-out, as shown in Fig. 13. There also was a considerable amount of resin adhering to the surface of the fibres, although the signi-

ficance of this is not obvious at present. Fig. 14 shows a region near the centre of the fracture surface. As is obvious from Fig. 12, the unbroken Kevlar 49 fibre layers had to be cut away in order to expose this fracture surface. The failure in this region exhibited more cleavage than near the tension surface, being more like that observed everywhere in the glass/epoxy hybrid, Type A, longitudinal impact specimens (Fig. 5).

### 5.5. Modulite 5206/Kevlar 49 hybrid-type B laminates

As indicated by the total impact energy values given in Table II, the longitudinal impact specimens exhibited a considerable amount of

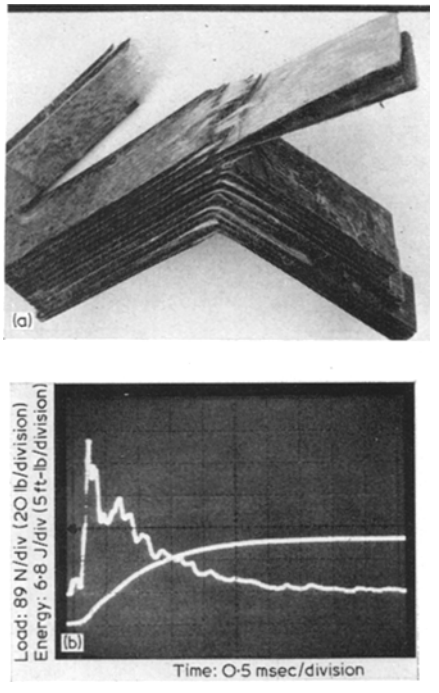


*Figure 15* Modulite 5206/Kevlar 49 hybrid, lay-up B, longitudinal impact, unnotched specimen. (a) Failed impact specimen, tension side at top; (b) instrumented impact load and energy waveforms.

notch sensitivity while the transverse impact specimens did not. Figs. 15 and 16 are photographs of a typical unnotched and notched specimen, respectively. In neither configuration did the Kevlar 49 third phase fibres, oriented in the 0° direction (along the beam axis), actually fail during impact. As in the case of the Modulite 5206/glass hybrid, type B, longitudinal impact specimens, the specimens became flexible enough

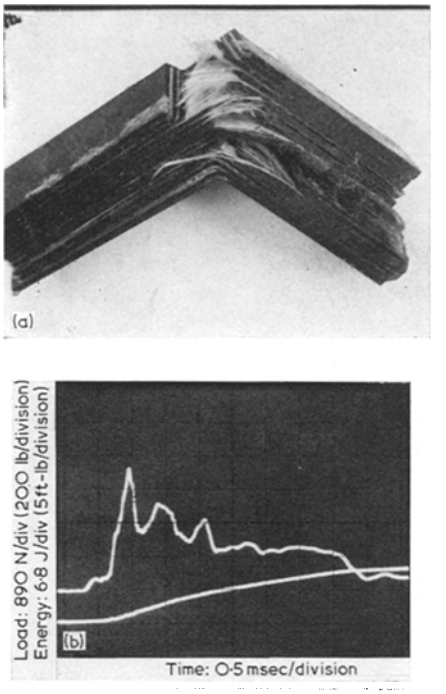


*Figure 16* Modulite 5206/Kevlar 49 hybrid, lay-up B, longitudinal impact, notched specimen. (a) Failed impact specimen, tension side on top; (b) instrumented impact load and energy waveforms.

during the latter stage of the impact process (because of gross delaminations and complete failure of all of the graphite/epoxy plies) to slip off of the support points. The Kevlar 49 plies were cut with a razor blade to permit examination of the graphite plies.

Fig. 17 shows a typical fracture surface in a 0° graphite/epoxy ply near the tension side of the unnotched specimen of Fig. 15. Most of the area was a flat cleavage surface, with occasional bundle pull-outs being observed fairly uniformly spaced across the width of the ply. The hole in the left half of Fig. 17 indicates a region where a bundle of fibres has pulled out. As in the case of lay-up A specimens, there also appeared to be a considerable amount of resin adhering to the fibre surfaces in the pull-out regions. SEM photographs taken normal to the fracture surface of the 90° plies of Modulite 5206 indicated good fibre/matrix bonding, few graphite fibres being visible. The 45° plies did indicate some fibre bundle pull-out; more than in the glass-reinforced lay-up B hybrid systems.

Fig. 18 shows a region of a 0° ply of Modulite 5206 right at the notch root of the specimen

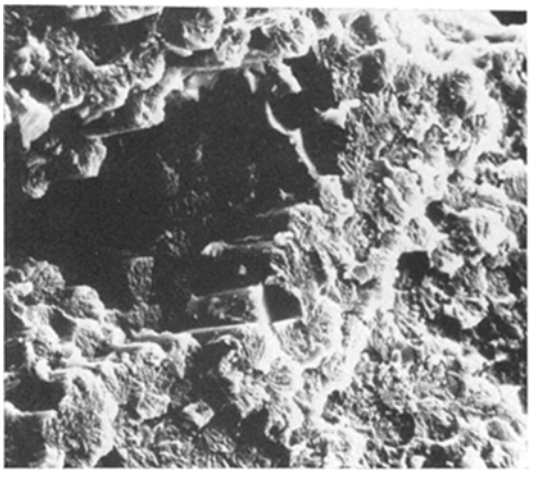

*Figure 17* Modulite 5206/Kevlar 49 hybrid, lay-up B, longitudinal impact, unnotched: 0° graphite/epoxy ply, near tension surface, × 1000.

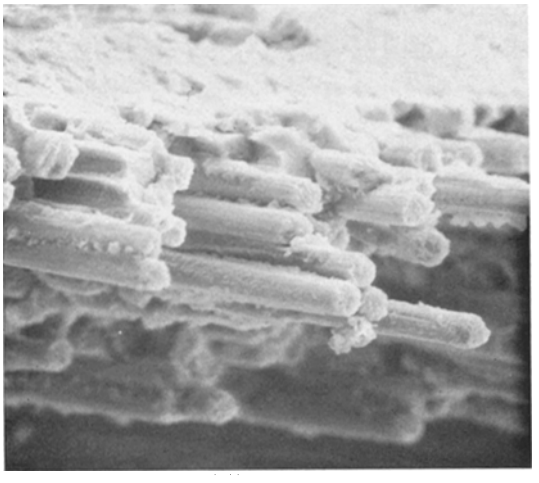

*Figure 18* Modulite 5206/Kevlar 49 hybrid, lay-up B, longitudinal impact, notched: notch shown at top of photo, delamination at bottom, × 600.

shown in Fig. 16. As in the case of the unnotched specimens of this material, the projection of the Kevlar 49 fibres above the mean surface made photography difficult, perhaps because the Kevlar 49 fibres shaded the Modulite 5206 plies during the gold vapour coating process. The lighter region along the upper edge of Fig. 18 is the surface of the notch root, which happened to cut into approximately one-half of the thickness of the 0° ply of Modulite 5206 shown. A − 45° ply was directly below this 0° ply, but is not seen because of a large delamination which separated it from the 0° ply. The edge of this delamination is shown along the bottom edge of Fig. 18.

The Modulite 5206/Kevlar 49 hybrid, type B laminate, longitudinal impact specimens exhibited the greatest amount of notch sensitivity in terms of effect on total impact energy absorbed. Hence, the primary purpose of carefully examining the notch root region of this specimen and the tension side of the unnotched but otherwise identical specimen was to look for indications of a difference in the failure mode.

There was little question that the micro failure modes were different. As can be seen in Fig. 18, there was a distinct pull-out of individual fibres and small groups of fibres all along the notch root. The very flat, cleavage failure exhibited by the unnotched specimen (Fig. 17) was totally absent. Note also that the macro failure modes were slightly different, as a comparison of Figs. 15 and 16 indicates. The unnotched specimens tended to delaminate more extensively at the tension surface; some of the outer plies are actually missing in Fig. 15. Away from the tension side, both failures are essentially very similar.

The transverse impact specimens, which did not exhibit a notch sensitivity in terms of energy absorbed, also did not exhibit a difference in macro failure mode. Both the notched and the unnotched specimens did fracture completely, in a manner similar to that observed in the Modulite 5206/glass hybrid, but with several additional gross delaminations being visible.

### 5.6. Modulite 5206/Nomex hybrid-type A laminates

Like all other lay-up A material combinations tested, the Nomex hybrid did not exhibit a notch sensitivity. The observed microfailure modes were essentially the same as previously described for the glass and Kevlar 49 (Fig. 17) hybrid systems.

The longitudinal impact specimens exhibited failures similar to that shown in Fig. 3 for the glass hybrid. However, the transverse specimens, both notched and unnotched, exhibited very little pull-out of Nomex/epoxy plies, unlike that shown in Fig. 4 for the glass hybrid. The failure planes were very flat, and essentially normal to the longitudinal axis of the specimen.

### 5.7. Modulite 5206/Nomex hybrid-type B laminates

Like type A laminates, the type B laminates

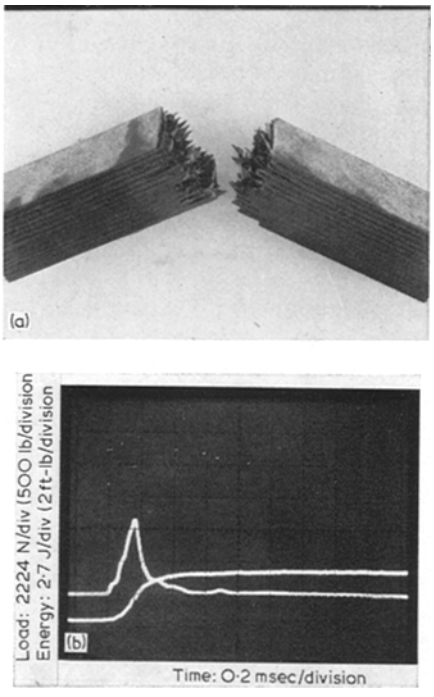


*Figure 19* Modulite 5206/Nomex hybrid, lay-up B, transverse impact, unnotched specimen. (a) Failed impact specimen, tension side at top; (b) Instrumented impact load and energy waveforms.

indicated no notch sensitivity. While the longitudinal type A laminates exhibited some gross delamination and the transverse laminates an almost perfect cleavage failure, i.e. a distinct difference in failure mode and a distinct difference in energy absorbed (see Table II), the failed longitudinal and transverse Type B specimens looked essentially the same. A typical failed specimen is shown in Fig. 19.

As can be seen, the gross failure mode of this hybrid system is relatively brittle in nature, with no gross delaminations occurring. The Nomex fibres failed completely during impact. There was typically some local pull-out of plies, as indicated in Fig. 19. However, these were almost exclusively the $\pm$ 45° graphite/epoxy plies. Very little Nomex was visible. On the microlevel, the fracture surfaces of the Modulite 5206 plies indicated amost no fibre or bundle pull-out, a very planar, cleavage failure being observed.

Fig. 20 is a close-up view of a Modmor II fibre fracture surface in a 90° ply of graphite/epoxy near the compression surface of the impact specimen of Fig. 19. The fracture surface is

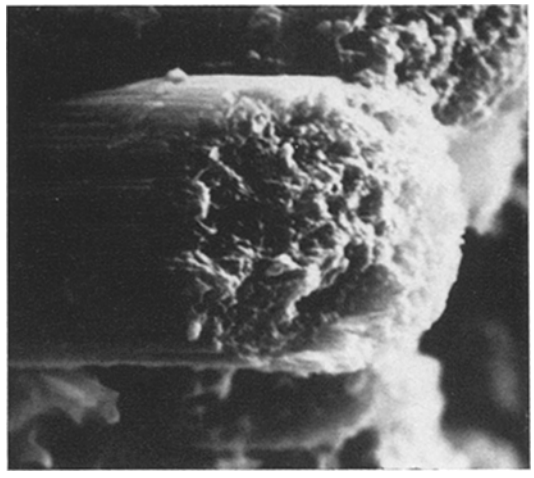

*Figure 20* Modulite 5206/Nomex hybrid, lay-up B, transverse impact, unnotched: 90° graphite/epoxy ply, × 6000.

uniform, and indicative of a tensile failure. This is in contrast to the fibre failure noted in Fig. 6.

## 6. Impact load–time traces

As described in Section 3, an instrumented impact testing technique was used, which provided a complete load–time trace during impact of each specimen. A representative sample of these traces are included in Figs. 1, 9, 12, 15, 16 and 19. Each of these traces is for the specific specimen shown in the same figure. Also shown on each of these plots is the trace of the energy, i.e. the integrated area under the load curve at any given time. The load curve is always that which peaks to a maximum value and then decays to zero. The energy curve rises monotonically to a maximum value. The divisions referred to on the axes are the square divisions shown in each plot. Since these plots are photographs taken directly from the oscilloscope, the energy values are not normalized by dividing by the specimen cross-sectional area as in Table II.

The humps in the load–time traces beyond peak load correspond roughly to the load build-up just prior to the occurrence of a major delamination. Note, for example, that there are no major or gross delaminations in the failed specimen of Fig. 19, and no significant humps in the corresponding load–time trace. Likewise, Fig. 1 indicates only one gross delamination, and one hump. The other specimens for which load–time traces are given did delaminate more

extensively, and this is reflected in the corresponding load–time trace.

The six instrumented impact load–time traces given in this paper are included for general information only. The interested reader is referred to [1] for a more detailed presentation and discussion of this type of macromechanical failure data.

## 7. Discussion

The primary purpose of this paper is to present a number of carefully obtained experimental measurements and observations relating to the impact behaviour of hybrid composite materials. These data have been assembled with an emphasis on factual information, and with a minimum of speculation.

The reason for the latter is that the indicated relations in the present paper between microfailure modes as determined by scanning electron microscopy and the gross behaviour of the various impact specimens in terms of energy dissipation and macrofailure modes do not support many of the generally proposed analytical theories which suggest that fibre-matrix debonding and fibre pull-out are the governing factors in impact energy absorption in composite materials [4-9]. More recently, Marston *et al.* [10] have also questioned these earlier concepts, presenting their own free surface energy theory, as applied in particular to boron-epoxy composites. Novak and De Crescente [11] have also raised a number of interesting questions concerning these various theories.

It would appear that much more experimental data of the type presented in the present paper will be needed in order to fully resolve these questions and lead to a rational and experimentally verifiable general failure theory. However, the continued use of these advanced experimental techniques such as instrumented impact testing and scanning electron microscopy should make it possible to verify or refute very quickly many of the general conceptual ideas of composite failure which have been postulated during the past decade.

## Acknowledgements

The investigation upon which this paper is based was sponsored by the Naval Air Systems Command, Washington, D.C., under the direction of Mr Maxwell Stander. The author wishes to thank Mr J. L. Perry of the Aeronutronic Division of Philco-Ford Corporation, who generated all the impact test data used here.

## References

1. J. L. PERRY, J. L. KIRKHART and D. F. ADAMS, Final Report, Naval Air Systems Command Contract N00019-73-C-0389, March 1974.
2. J. L. PERRY, M. L. DAMOTH and J. P. POPE Final Report, Naval Air Systems Command Contract N000 19-71-C-0166, May 1973.
3. J. L. PERRY and D. F. ADAMS, *Composites*, in press.
4. J. COOK and J. E. GORDON, *Proc. Roy. Soc. (Lond.)* **A282** (1964) 508.
5. A. KELLY, "Strong Solids" (Oxford University Press, 1966).
6. J. O. OUTWATER and M. C. MURPHY, 24th Annual Technical Conference, Reinforced Plastics/Composites Division, The Society of the Plastics Industry, Inc, paper IIC (1969).
7. M. PIGGOTT, *J. Mater. Sci.* **5** (1970) 669.
8. A. KELLY, *Proc. Roy. Soc. (Lond.)* **A299** (1967) 508.
9. P. W. R. BEAUMONT and B. HARRIS *J. Mater. Sci.* **7** (1972) 1265.
10. T. U. MARSTON, A. G. ATKINS D. F. FELBECK, *ibid* **9** (1974) 447.
11. R. C. NOVAK and M. A. DE CRESCENTE ASTM STP 497 (1972) p. 311.

Received 31 December 1974 and accepted 12 February 1975.